Transcriptome Sequencing Reveals Sex Differences in Human Meniscal Cell Response to Estrogen Based on Dosing Kinetics

Kelsey E. Knewtson[1], Jesus G. Gonzalez Flores[2], Donna M. Pacicca[3,4], Jennifer L. Robinson[1,2]

1. Chemical and Petroleum Engineering Department, University of Kansas, Lawrence, KS

2. Bioengineering Program, University of Kansas, Lawrence, KS

3. Children's Mercy Hospital, Kansas City, MO

4. University of Missouri-Kansas City, School of Dentistry, Kansas City, MO

Corresponding Author

Jennifer L. Robinson, PhD

1530 West 15th Street Room 4132

Lawrence, KS 66045

Tel: (785) 864-0298

jlrobinson@ku.edu

Running Title

Estrogen affects meniscus gene expression

Author Contributions

K.K. analyzed the data and wrote the manuscript. J.G.F. designed and performed the experiment and reviewed the manuscript. D.P. provided critical interpretation of the data and revised the manuscript. J.R. designed the experiment, supervised the study, and wrote the manuscript. All authors have read and approved of the submitted manuscript.

ABSTRACT: Osteoarthritis is a disease marked by progressive and irreversible hyaline cartilage and fibrocartilage breakdown that affects the lives of millions of patients worldwide. Female sex and menopause are both risk factors for knee osteoarthritis, indicating that estrogen could play a role in this disease. In this study, RNA sequencing was used to determine the effects of estrogen treatment on human meniscal cells. Differences in the number and type of differentially expressed genes were seen based on donor sex, estrogen dose, and dosing kinetics. Significantly more differentially expressed genes were seen from male meniscal cells in response to all dosing conditions compared to female cells. Importantly, more genes were differentially expressed in cells treated with continuous dosing of estrogen, which has been shown to stimulate genomic estrogen signaling, as compared to pulsed dosing. Additionally, functional enrichment analysis revealed that many genes of the extracellular matrix, which is important for joint health and injury repair, were differentially expressed. Overall, this initial study lays the groundwork for future avenues to pursue the effect of estrogen delivery on regenerative pathways. This critical analysis will then inform the design and implementation of estrogen replacement therapies to promote meniscal health and reduce the onset of osteoarthritis.

Keywords: estrogen treatment, meniscus tissue, sex differences, RNA sequencing

INTRODUCTION

An estimated 250 million people have knee osteoarthritis (OA) worldwide,[1] with more than 25 million cases in the United States alone.[2] Patients experience progressive and irreversible cartilage breakdown that leads to pain, immobility, and eventual joint failure. Meniscal tears are the most prevalent intra-articular knee injury and pose significant risk in the development of

48 OA.[3] Knee OA is more common and severe in women than in men, especially post-menopause.[4]
49 Also, tears of the meniscal body are more common in women than in men.[5] Further, recent
50 epidemiological studies have found that meniscal injury rates are higher in female high school
51 athletes than in males competing in comparable sports,[6] and that females require repeat meniscal
52 repair surgeries 2.2x more frequently.[7] These data suggest that sex hormone levels, including
53 estrogen, may play a role in meniscal injury and repair.

54 Estrogen is required for joint health and is used as a therapeutic for joint degenerative
55 conditions. Several studies have found a protective effect of estrogen replacement therapy (ERT)
56 against the development and progression of knee OA in post-menopausal women; however, the
57 effects were modest and did not reach significance.[8-10] Treatment with estrogen or selective
58 estrogen receptor modulators has been shown to improve OA symptoms in humans in some
59 studies, but the results are mixed and inconclusive.[11] While clinical data suggests estrogen
60 protects the knee joint and reduces OA, there is a dearth of *in vitro* and preclinical studies
61 investigating the role of estrogen on meniscal health and repair. A better understanding of the
62 effects of estrogen treatment on the knee is needed to develop therapies to improve joint health in
63 different populations.

64 The physiological effects of estrogen vary depending on concentration and dosing
65 kinetics. High and low concentrations of estrogen are known to have opposite effects on
66 inflammation,[12] gene expression,[13] and stem cell proliferation.[14] Specific 17β-estradiol (E2)
67 effects are dose-dependent and differ between tissues.[15] Additionally, several studies have found
68 that the effect of estrogen varies based on dosing kinetics both *in vitro*[16; 17] and *in vivo*.[18]
69 Typically, estrogen exerts its effects on cells by activating the nuclear estrogen receptors alpha
70 and beta, which then regulate transcription of many genes. However, it is known that estrogen

71 can also have quicker, non-genomic effects on cells.[19] There is evidence that controlling dosing
72 kinetics can control the type of response elicited.[16] Conversely, others have found that if total
73 hormone exposure is kept constant, dosing kinetics do not alter the effects of estrogen.[20]
74 The intricacies of the effects of estrogen are significant given the different levels of
75 estrogen seen in patients of different sexes and stages of life and the different doses and delivery
76 routes used for ERT. Serum estradiol levels in healthy, menstruating women range from 40-400
77 pg/mL (150-1,500 pM) depending on the phase of the menstrual cycle,[21] while levels in pregnant
78 women range from 2,000-20,000 pg/mL (7,300-73,000 pM) depending on trimester.[22] Post-
79 menopausal women typically have serum estradiol levels below 15 pg/mL (60 pM).[21] Healthy
80 men under age 55 average serum estradiol levels less than 40 pg/mL (150 pM),[21; 23] and these
81 levels decrease as men age and their testosterone levels decrease.[23] Average serum levels of
82 estradiol achieved by ERT typically range from 20-100 pg/mL.[24] Less data is available on
83 synovial fluid (SF) estradiol levels, which is the most pertinent data for tissues such as the
84 meniscus. The data available for SF is mostly limited to older patient populations with OA or
85 rheumatoid arthritis (RA). These studies have found estradiol SF levels ranging from 15-54
86 pg/mL (60-200 pM) in male and female patients, with higher levels typically seen in RA patients
87 than in OA patients.[25; 26] Though these levels cannot be applied to other populations, these
88 studies did find strong, positive linear correlations between serum and SF estradiol levels that
89 could be applicable to other groups. In terms of ERTs, each treatment type (e.g. formulation and
90 deployment form) is associated with a different hormone exposure level and kinetic profile. For
91 example, though a 50 μg/day transdermal reservoir patch, 2 mg oral tablet, and 300 μg nasal
92 dose of E2 all provide similar 24 h systemic exposures (1080-1400 pg*h/ml), they each have a
93 unique kinetic profile ranging from continuous over days with a transdermal patch to pulsed over

94 hours with a nasal delivery route.[27] Further studies are needed to understand the effects of
95 estrogen concentration and dosing kinetics on tissues of interest from different patient
96 populations.

97 In this study, we aimed to both determine sex differences and the role of concentration
98 and dosing kinetics on human knee meniscal cell gene expression changes in response to
99 estrogen treatment. Cells were isolated from the menisci of two age-matched donors, one of each
100 sex, and treated with two concentrations of 17β-estradiol (E2) under pulsed and continuous
101 conditions. Messenger RNA sequencing (RNA-Seq) was then used to determine differentially
102 expressed genes as a function of the E2 treatment groups. Results from this study will inform
103 future work on developing a mechanistic understanding of estrogen delivery conditions on cell
104 and tissue response to aid in design and development of treatments for knee injury based on
105 patient sex.
106

107 **METHODS**

108 **Cells and Treatment**

109 The experimental design and workflow are illustrated in Figure 1. Human meniscal tissue was
110 received from the National Disease Research Interchange (NDRI). Cells were harvested from the
111 medial meniscus of a human cadaveric male (Black) and a female (Caucasian) (both 47-year
112 old). Briefly, whole menisci were cut into small pieces (1-2 mm) and digested in DMEM
113 (11996-065, Gibco, Carlsbad, CA) containing 2% penicillin/streptomycin (15140-122, Gibco,
114 Carlsbad, CA) and 3 mg/mL collagenase type I (17100-017, Gibco, Carlsbad, CA) at 37 °C and
115 60 rpm for 16 h. Solutions were filtered through Swinnex Filter Holders (25 mm, SX0002500,
116 Sigma-Aldrich, St. Louis, MO) loaded with Spectra Mesh Nylon Filters (30 μM, 888-13681,

117 Spectrum Chemical Manufacturing Corporation, New Brunswick, NJ) to remove undigested
118 tissue. Cells were then cultured in T75 tissue culture treated flasks in DMEM supplemented with
119 10% Premium FBS (511150, Atlanta Biologicals, Minneapolis, MN) and 1%
120 penicillin/streptomycin. After reaching confluency, cells were passaged using trypsin (T4174,
121 Sigma, St. Louis, MO, diluted to 1x before use) and seeded into T225 tissue culture treated
122 flasks. When passage 1 cells reached 70-80% confluency, cells were washed with PBS (20012-
123 207, Gibco, Carlsbad, CA) and cultured in phenol red-free DMEM (pfDMEM, 31053-028,
124 Gibco, Carlsbad, CA) with 15% charcoal/dextran treated FBS (S11650, Atlanta Biologicals,
125 Minneapolis, MN) for 3 days to starve them of endogenous hormones. Cells were then passaged
126 and seeded at 10,000 cells/cm^2 in 24 well plates in pfDMEM and allowed to adhere overnight.
127 The next day, cells were treated in triplicate with 17β-estradiol (E2, E2758, Sigma, St. Louis,
128 MO) in pfDMEM supplemented with 15% charcoal/dextran treated FBS and 1%
129 penicillin/streptomycin under pulsed or continuous dosing. For pulsed dosing, cells were
130 exposed to E2 (0, 24, or 240 μM) for 1 h, after which the E2 media was replaced with E2-free
131 media for 23 h. This pattern was repeated for a total of 72 h. For continuous dosing, cells were
132 exposed to E2 (0, 1, or 10 μM) for the entire treatment period of 72 h. The different
133 concentrations used for pulsed compared to continuous dosing were used so that the total 24 h
134 exposure was identical between groups, as reported previously.[16; 17; 20] The concentrations used
135 were chosen to be above normal physiological levels in order to elicit a significant response.
136 Further, 1 μM is predominantly used as a high concentration in *in vitro* estrogen dosing studies.
137 Different dosing kinetics were used to mimic those seen with different types of estrogen
138 replacement therapies such as pulsed from nasal doses of E2 and continuous from transdermal
139 patches.

140

141 **RNA Extraction, cDNA Library Construction, and Sequencing**

142 After 72 h, cells were collected in TRIzol, and total RNA was purified using the manufacturer's
143 protocol. DNA was removed using a DNA-*free* DNA Removal Kit (AM1906, Life
144 Technologies, Grand Island, NY). Total RNA samples were quality checked with a Qubit Assay
145 and Agilent TapeStation for quantity and quality, respectively. All RNA preps had an estimated
146 RIN value that ranged from 8.8-10. Sequencing libraries were constructed using the NEBNext
147 Ultra II Directional RNA Library Prep Kit for Illumina (E7760, New England BioLabs, Ipswich,
148 MA). The library preps were started with 92-1000 ng of total RNA. The sequencing library
149 construction process includes mRNA purification with polyA selection beads, fragmentation to
150 inserts of ~200 bp, strand specific cDNA synthesis, end repair, 3' end adenylation, adapter
151 ligation, and PCR amplification. The constructed sequencing libraries were validated and
152 quantified with Qubit and TapeStation assays. Each library was indexed with a barcode sequence
153 and sequenced in a multiplexed fashion. An Illumina NextSeq 550 system at the University of
154 Kansas's Genome Sequencing Core was used to generate single-end, 100-base sequence reads
155 from the libraries.

156

157 **Data Processing**

158 Base calling was carried out by the instrument Real Time Analysis (RTA) software. The base
159 call files (bcl files) were demultiplexed and converted to compressed FASTQ files by bcl2fastq2.
160 Raw reads were filtered using fastp,[28] retaining only reads longer than 40 nucleotides. Processed
161 reads were then pseudoaligned to the human reference transcriptome (ensembl.org, release 97,
162 build GRCh38) using kallisto,[29] employing 100 bootstraps to estimate transcript abundance.

163 tximport[30] was then used to import kallisto transcript abundance estimates into DESeq2[31]
164 for differential expression analysis. Within DESeq2, a series of pairwise likelihood ratio tests to
165 identify genes showing differential gene expression, considering genes to be differentially
166 expressed for a given test if they survived a 5% False Discovery Rate criterion, was conducted.
167 GraphPad Prism 8 was used to generate volcano plots by plotting the $\log_2$FoldChange against the
168 adjusted P value. Venny 2.1[32] was used to generate Venn diagrams of the differentially expressed
169 genes with adjusted p values (padj) < 0.05. Venn diagrams were then redrawn using Adobe
170 Illustrator to allow for color control. Significant results were further analyzed using the Search
171 Tool for the Retrieval of Interacting Genes/Proteins (STRING)[33] to detect protein-protein
172 interactions using the confidence view to display connection thickness based upon strength of the
173 supporting data. Functional enrichment analysis was performed within STRING, with databases
174 and categories selected based upon first significance and then ability to highlight gene clusters.
175 The Database for Annotation, Visualization and Integrated Discovery (DAVID)[34] was used for
176 further functional enrichment analysis with the human genome used as the background. The
177 Gene Ontology Cellular Component database was used within the Functional Annotation Chart
178 function of DAVID. Heat maps were generated using GenePattern.[35] To generate the list of
179 extracellular matrix genes, the genes identified within this category by DAVID for each
180 treatment group were compiled into a master list of ECM genes. The $\log_2$FoldChange for these
181 genes were then gathered from each treatment group and used uploaded to the Heat Map Image
182 module of GenePattern. Column and row sizes were set to 128 pixels, the color scheme was
183 globally normalized, and color gradient was not used.
184
185 **RESULTS**

186 **Male Meniscal Cells Respond More Robustly to Estrogen Treatment**

187 The number of genes in each treatment group that were differentially expressed (DEGs) as
188 compared to the sex-matched no E2 control was plotted in terms of E2 concentration relative to
189 physiological concentrations (Figure 2). This revealed that male cells responded more strongly to
190 E2 treatment than female cells. In general, more DEGs were seen from groups treated with
191 continuous dosing than for groups treated with pulsed dosing, though the male high dose pulsed
192 group had the most DEGs of all treatment groups. Additionally, within the female treatment
193 groups, there were greater differences in the number of DEGs based on dosing kinetics than on
194 concentration. In males, E2 concentration had a large effect on DEG count for the pulsed groups,
195 an effect that does not trend with the other comparisons in which concentration did not play as
196 significant a role when controlling for kinetics.

197 Volcano plots were generated to visualize the number of DEGs in each treatment group
198 in terms of fold change and adjusted P value (Figure 3A). These plots show that in most
199 treatment groups, the majority of DEGs had a $\log_2$FoldChange between -2 and 2, though most
200 groups had at least one gene that fell far outside this range. Examples include POLR2J3 in the
201 female high dose pulsed group ($\log_2$FoldChange -7.98) and GNL1 in the male high dose pulsed
202 group ($\log_2$FoldChange 9.94)

203 The Venn diagrams in Figure 3B illustrate more overlap in the DEGs of the male
204 treatment groups compared to the female groups. In fact, 230 genes were common to all 4
205 groups. Further analysis of these overlapping genes can be seen in Table S1 and Figure S1. This
206 analysis revealed that many groups of genes, including those of the extracellular matrix (ECM),
207 were enriched in this set and that there were many protein-protein interactions among the genes.
208 The highest overlap in DEGs occurred between the male high dose groups, where 823 DEGs

209 were seen in both groups (262 genes that only overlap between the high dose groups and 561 that
210 also overlap with other groups). Comparatively, the highest overlap in female meniscal cell
211 treatment was seen in the continuous treatment groups, where 20 DEGS were seen in both
212 groups.
213
214 **Types of DEGs Differ Based on Estrogen Dosing Concentration and Kinetics and Sex**
215 The DEGs from each continuous dosing treatment group were then analyzed using STRING[33]
216 (Figure 4). Additional constraints based on log_2FoldChange were used to limit DEGs to a
217 reasonable number for visualization and to highlight those with greater fold changes compared to
218 control. STRING analysis of the other treatment groups and images without log_2FoldChange
219 constraints can be found in Figures S2-S4. Functional enrichment analysis was also performed
220 within STRING, as indicated by the color coding of certain proteins. This revealed that the
221 DEGs of both female continuous dosing groups were enriched for proteins of the ECM, which is
222 of interest for its importance to joint healing. In the male continuous groups, low dose resulted in
223 DEGs related to metabolic pathways involving nitrogen and high dose resulted in DEGs
224 involved in gene expression and thyroid hormone signaling pathways.
225
226 **Conservation of DEGS in Continuous Treatment Groups of Both Sexes**
227 Additional analysis was done to compare the effects of the same treatment in different sexes
228 (Figure 5). Venn diagrams (Figure 5a) illustrate that relatively few DEGs were common between
229 the same treatment of different sexes, with the most overlap occurring between the high dose
230 continuous groups. Interestingly, in the continuous dosing groups with low and high dose, four
231 genes are conserved in both female and male cells indicating similar control of estrogen on the

232 transcription of these genes. The proteins for which these genes encode function as facilitators of
233 transport across cell membranes (*SLC7AA1 and ABCC1),* protease that functions to cleave
234 insulin-like growth factor binding proteins necessary for bone formation, inflammation, wound
235 healing, and fertility (*PAPPA1 and 2)*, and transcription factor and ubiquitin binding (*UBXN7)*.
236 The complete list of these overlapping DEGs can be found in Table S2. DAVID analysis (Figure
237 5b) revealed several groups enriched in these datasets compared to the human genome including
238 extracellular exosomes in the low dose continuous treatments and extracellular space in the high
239 dose continuous groups. STRING analysis (Figure 5c) illustrated that there were few protein-
240 protein interactions between these genes. However, interactions controlling cell cycle processes
241 (PAPPA/PCNA/TMSB4X) and TGFβR1/SMAD9, both important for meniscus cell proliferation
242 and phenotype, were highlighted in the high dose continuous groups of both sexes.
243 Overlapping DEGs as a function of treatment in the female groups are shown in Figure 6.
244 Overall, continuous dosing exhibited the most conserved DEGs with estrogen concentration
245 (Figure 6a). In looking at the pathway enrichment (Figure 6b) and protein-protein interactions
246 (Figure 6c), genes involved in repair and homeostasis of the ECM are reported. All 20 DEGs of
247 this group are shown with their expression in all other groups in the heat map in Figure 6d. The
248 major genes regulated were all protein coding genes that are implicated in cell-cell signaling
249 (*ACKR4, CLDN11),* or cell differentiation (*PAMR1, S100A4, and S100A5*). A full list of these
250 genes can be found in Table S3.
251
252 **DEGS Related to the Extracellular Matrix from Estrogen Treatment**
253 Functional enrichment analysis using DAVID[34] showed that the types of genes enriched varied
254 depending on donor sex, E2 dose, and dosing kinetics (Figure 7). Of interest for joint healing,

genes of the ECM, highlighted in red, were enriched in all treatment groups except the female pulsed dosing groups. Genes related to extracellular exosomes and focal adhesion were enriched in all the male treatment groups plus the female low dose continuous group. Membrane, cytoplasm, and cytosol genes were enriched in all male treatment groups but none of the female treatment groups. Genes of the actin cytoskeleton were only enriched in both male low dose groups. Nucleus genes were enriched in all male groups except low dose pulsed. Genes of the basement membrane, extracellular region, extracellular space, collagen trimer, and endoplasmic reticulum lumen were enriched in both female continuous dosing groups but not in any of the male treatment groups.

The importance of estrogen in promoting new extracellular matrix for fibrocartilage tissue regeneration and homeostasis has been previously detailed.[36] For this reason, the relative expression of genes within the ECM category from each treatment group are illustrated in a heat map in Figure 8. Separate heat maps for both sexes, doses, and dosing kinetics can be found in Figures S5-S7. The expression levels of many genes were either up- or down-regulated in all treatment groups. For example, ABI3BP, ADAMTS3, CANX, CDON, FBN1 and 2, LOXL2, LTBP2, TIMP2 and 3, and many collagens were down-regulated in all treatment groups and CALR, CFL1, CRIP2, LOXL1, LTBP3 and 4, and TNXB were up-regulated in all groups. Others such as ACTG1, COL14A1, COL7A1, HMCN1, mATN2, OGN, and PFKP were split by donor sex. No clear patterns were present based on low versus high dose, except for the ribosomal proteins in male treatment groups. Of particular interest to cartilage and fibrocartilage, COMP, POSTN, and TGFB1 and 3 were differentially regulated based on sex and estrogen dosing kinetics.

278 **Discussion**

279 A number of microarray and sequencing studies have provided important insight on
280 transcriptome differences in the meniscus including avascular meniscus that heals poorly,[37] in
281 meniscus from patients with and without osteoarthritis,[38] the progenitor cell phenotype that may
282 reduce osteoarthritis,[39] and single-cell sequencing to define unique meniscal progenitor
283 populations that are critical to maintain tissue health and reduce degeneration.[40] Building off this
284 body of work, this study focuses on transcriptome differences between male and female tissue
285 that will inform sex differences in natural aging and inform the role of sex hormones in repair
286 and homeostasis.

287 There is evidence that estrogen replacement therapy can reduce OA incidence and
288 symptoms.[8-11] ERT can also prevent and treat osteoporosis and osteoarthritis. Unfortunately,
289 ERT is not without risk and can have negative off-target effects. Oral use of ERT increases the
290 risk of venous thromboembolism in post-menopausal women.[41] Combination use of estrogen
291 plus progestin, and to a lesser extent estrogen alone, is linked with an increased risk of breast
292 cancer in some studies.[42; 43] The results presented here contribute to the pool of evidence
293 supporting the importance of estrogen dose and kinetics for achieving the desired results in
294 different patient populations. Further studies could lead to knowledge about estrogen dose and
295 kinetics that are needed to develop safe and effective treatments for knee injury and mitigate the
296 need for systemic dosing at high concentrations needed to hit therapeutic dose that lead to
297 deadly, off-target effects.

298 While more DEGs were reported in all of the male treatment groups, a hypothesized
299 effect due to the relative naivety of the male cells to high estrogen doses, an important finding is
300 the interplay between concentration and kinetics in both groups. In most cases, there were more

301 DEGs seen in treatment groups with continuous dosing than with pulsed dosing. This
302 corresponds with the findings of Simoncini *et. al.* that continuous E2 dosing of human umbilical
303 vein endothelial cells (HUVECs) leads to heavier E2 signaling through the traditional genomic
304 pathways than pulsed dosing.[16] In contrast, Cavailles *et. al.* found no difference in the effects of
305 pulsed compared to continuous estrogen dosing on the expression levels of 3 estrogen-responsive
306 genes.[20] This inconsistency can possibly be explained by the different scopes of the studies and
307 different concentrations of E2 used. Another study found more DEGs in HUVECs treated with
308 pulsed estrogen than those treated with continuous estrogen,[17] in direct contradiction to the
309 current study. A possible explanation for this is the differential response to estrogen dosing
310 kinetics based on tissue type seen by Otto *et. al.*[18] Interestingly, with continuous dosing,
311 concentration did not play a major role in total DEGs whereas concentration did play a
312 significant role with pulsed dosing. This evidence may indicate the ability to achieve similar
313 transcriptional effects using continuous dosing at lower concentrations which is important to
314 reduce the negative, off-target effects to other tissues in ERT. Also, in the female groups, pulsed
315 dosing resulted in lower total DEGs whereas the total DEGs was a function of concentration in
316 the male groups. Overall, it is likely that continuous dosing is required for the robust
317 transcriptional changes necessary for remodeling and homeostasis to maintain meniscal health
318 and reduce OA.
319 Functional enrichment analysis using DAVID and STRING revealed that the types of
320 genes enriched varied by donor sex, E2 dose, and dosing kinetics. Genes related to the
321 extracellular matrix were enriched in all groups except the female pulsed groups. It is also of
322 interest that the DEGs common to both male and female cells are related to the extracellular
323 matrix. While all of the differentially expressed collagens and tissue inhibitors of

324 metalloproteinases (TIMPs) are downregulated within all treatment groups, growth factors such
325 as in the TGFβ family are upregulated in all male groups and in the female pulsed groups. This is
326 information that must be pursued in future studies as TGFβ3 is a major growth factor in
327 meniscus remodeling and repair[44-46] and activation of this protein enhances differentiation ability
328 of meniscus progenitors to chondrogenic-like avascular tissue.[39; 47] Additionally, TNXB, LTBP3,
329 and LTBP4, genes that have each been shown to play a role in the activation, availability, and/or
330 signaling of TGFβ[48; 49], are all upregulated in all groups. LTBP2, another gene in the LTBP
331 family, is down-regulated, but it is also the only one in the family that does not bind to latent
332 TGFβ.[49] TNXB is also important for the correct assembly of other matrix molecules and wound
333 healing.[49] Further, this study is only assessing transcriptional changes after 72 hours and thus is
334 likely not capturing all of the transcriptional changes occurring with E2 treatment.
335 There are limitations to the current study that should be considered. This study was
336 performed using 2D culture methods, which are known to promote a more fibroblast-like
337 phenotype of the meniscal fibrochondrocytes[37; 50] and thus will indicate more of the fibroblast-
338 like cell response to estrogen. Additionally, this study was performed using cells isolated from
339 only 2 donors, both 47-years old. It is likely that these cells had relatively limited remodeling
340 capability due to the age of the donors. Furthermore, the 2 donors were of different races (Black
341 and Caucasian), which could have been a complicating factor. Future studies on 3D cultures
342 using tissue from more donors of different ages and more concentrations of estrogen could be
343 very informative to elucidate more conclusive effects of estrogen on the meniscus and for the
344 development of treatments for knee injury.
345
346 **Conclusions**

347 Overall, the estrogen dosing kinetics played a more significant role on total DEG compared to
348 estrogen concentration in both sexes. There were only four DEGs conserved across sexes in both
349 low and high concentrations in continuous dosing illustrating that meniscus cell transcriptional
350 response to estrogen signaling is significantly different between male and females. Future work
351 will expand on this initial data set to probe the effect of specific pathways, such as TGF-β3
352 known to promote meniscus healing, to provide clear insight into the role estrogen plays on
353 meniscus regeneration and homeostasis. Overall, this initial study lays the groundwork for
354 future avenues to pursue the effect of estrogen delivery on regenerative pathways to inform the
355 design and implementation of ERT therapies to promote meniscal health and reduce the onset of
356 osteoarthritis.
357

358 **Acknowledgments**

359 The authors acknowledge the use of tissues procured by the National Disease Research
360 Interchange (NDRI) with support from NIH grant U42OD11158. The authors want to thank
361 Brittney Smith and Jennifer Hackett at the KU Genome Sequencing Center (GSC) for
362 completing the sequencing (NIH NIGMS P20GM103638) and Boryana Koseva and Stuart
363 Macdonald of the K-INBRE Bioinformatics Core for providing computational support (NIH P20
364 GM103418). Further, the authors are appreciative of the insight and analysis feedback from Dr.
365 Emily Farrow, director of laboratory operations at the Genome Center at Children's Mercy
366 Hospital. This work was supported by startup funds from the University of Kansas (JR) and NIH
367 NIGMS P20GM103638 (KK, JGG, and JLR). This manuscript appears in the pre-print server
368 bioRxiv (2020.04.27.064451, https://www.biorxiv.org/content/10.1101/2020.04.27.064451v1).
369

370 **References**

371 1. O'Neill TW, McCabe PS, McBeth J. 2018. Update on the epidemiology, risk factors and
372 disease outcomes of osteoarthritis. Best Pract Res Clin Rheumatol 32:312-326.
373 2. Zhang Y, Jordan JM. 2010. Epidemiology of osteoarthritis. Clin Geriatr Med 26:355-369.
374 3. Englund M, Roos EM, Lohmander LS. 2003. Impact of type of meniscal tear on
375 radiographic and symptomatic knee osteoarthritis: a sixteen-year followup of
376 meniscectomy with matched controls. Arthritis Rheum 48:2178-2187.
377 4. Srikanth VK, Fryer JL, Zhai G, et al. 2005. A meta-analysis of sex differences
378 prevalence, incidence and severity of osteoarthritis. Osteoarthritis Cartilage 13:769-781.
379 5. Ding C, Martel-Pelletier J, Pelletier JP, et al. 2007. Meniscal tear as an osteoarthritis risk
380 factor in a largely non-osteoarthritic cohort: a cross-sectional study. J Rheumatol 34:776-
381 784.
382 6. Mitchell J, Graham W, Best TM, et al. 2016. Epidemiology of meniscal injuries in US
383 high school athletes between 2007 and 2013. Knee Surg Sports Traumatol Arthrosc
384 24:715-722.
385 7. Patel NM, Mundluru SN, Beck NA, et al. 2019. Which Factors Increase the Risk of
386 Reoperation After Meniscal Surgery in Children? Orthop J Sports Med
387 7:2325967119842885.
388 8. Hannan MT, Felson DT, Anderson JJ, et al. 1990. Estrogen use and radiographic
389 osteoarthritis of the knee in women. The Framingham Osteoarthritis Study. Arthritis
390 Rheum 33:525-532.

391 9. Zhang Y, McAlindon TE, Hannan MT, et al. 1998. Estrogen replacement therapy and
392 worsening of radiographic knee osteoarthritis: the Framingham Study. Arthritis Rheum
393 41:1867-1873.
394 10. Hart DJ, Doyle DV, Spector TD. 1999. Incidence and risk factors for radiographic knee
395 osteoarthritis in middle-aged women: the Chingford Study. Arthritis Rheum 42:17-24.
396 11. Xiao YP, Tian FM, Dai MW, et al. 2016. Are estrogen-related drugs new alternatives for
397 the management of osteoarthritis? Arthritis Res Ther 18:151.
398 12. Straub RH. 2007. The complex role of estrogens in inflammation. Endocr Rev 28:521-
399 574.
400 13. Koelling S, Miosge N. 2010. Sex differences of chondrogenic progenitor cells in late
401 stages of osteoarthritis. Arthritis Rheum 62:1077-1087.
402 14. Lee WJ, Lee SC, Lee JH, et al. 2016. Differential regulation of senescence and in vitro
403 differentiation by 17beta-estradiol between mesenchymal stem cells derived from male
404 and female mini-pigs. J Vet Sci 17:159-170.
405 15. Fontaine C, Buscato M, Vinel A, et al. 2020. The tissue-specific effects of different
406 17beta-estradiol doses reveal the key sensitizing role of AF1 domain in ERalpha activity.
407 Mol Cell Endocrinol 505:110741.
408 16. Simoncini T, Fornari L, Mannella P, et al. 2005. Differential estrogen signaling in
409 endothelial cells upon pulsed or continuous administration. Maturitas 50:247-258.
410 17. Li J, Wang H, Johnson SM, et al. 2008. Differing transcriptional responses to pulsed or
411 continuous estradiol exposure in human umbilical vein endothelial cells. J Steroid
412 Biochem Mol Biol 111:41-49.

413 18. Otto C, Kantner I, Nubbemeyer R, et al. 2012. Estradiol release kinetics determine tissue
414 response in ovariectomized rats. Endocrinology 153:1725-1733.
415 19. Azuma K, Inoue S. 2012. Genomic and non-genomic actions of estrogen: recent
416 developments. Biomol Concepts 3:365-370.
417 20. Cavailles V, Gompel A, Portois MC, et al. 2002. Comparative activity of pulsed or
418 continuous estradiol exposure on gene expression and proliferation of normal and
419 tumoral human breast cells. J Mol Endocrinol 28:165-175.
420 21. Sluss PM, Hayes FJ, Adams JM, et al. 2008. Mass spectrometric and physiological
421 validation of a sensitive, automated, direct immunoassay for serum estradiol using the
422 Architect. Clin Chim Acta 388:99-105.
423 22. Schock H, Zeleniuch-Jacquotte A, Lundin E, et al. 2016. Hormone concentrations
424 throughout uncomplicated pregnancies: a longitudinal study. BMC Pregnancy Childbirth
425 16:146.
426 23. Decaroli MC, Rochira V. 2017. Aging and sex hormones in males. Virulence 8:545-570.
427 24. Stanczyk FZ, Clarke NJ. 2014. Measurement of Estradiol—Challenges Ahead. The
428 Journal of Clinical Endocrinology & Metabolism 99:56-58.
429 25. Rovensky J, Radikova Z, Imrich R, et al. 2004. Gonadal and adrenal steroid hormones in
430 plasma and synovial fluid of patients with rheumatoid arthritis. Endocr Regul 38:143-
431 149.
432 26. Richette P, Laborde K, Boutron C, et al. 2007. Correlation between serum and synovial
433 fluid estrogen concentrations: comment on the article by Sowers et al. Arthritis Rheum
434 56:698; author reply 698-699.

435 27. Devissaguet JP, Brion N, Lhote O, et al. 1999. Pulsed estrogen therapy: pharmacokinetics
436 of intranasal 17-beta-estradiol (S21400) in postmenopausal women and comparison with
437 oral and transdermal formulations. Eur J Drug Metab Pharmacokinet 24:265-271.
438 28. Chen S, Zhou Y, Chen Y, et al. 2018. fastp: an ultra-fast all-in-one FASTQ preprocessor.
439 Bioinformatics 34:i884-i890.
440 29. Bray NL, Pimentel H, Melsted P, et al. 2016. Near-optimal probabilistic RNA-seq
441 quantification. Nat Biotechnol 34:525-527.
442 30. Soneson C, Love MI, Robinson MD. 2015. Differential analyses for RNA-seq: transcript-
443 level estimates improve gene-level inferences. F1000Res 4:1521.
444 31. Love MI, Huber W, Anders S. 2014. Moderated estimation of fold change and dispersion
445 for RNA-seq data with DESeq2. Genome Biol 15:550.
446 32. Oliveros JC. 2007-2015. Venny-An interactive tool for comparing lists with Venn's
447 diagrams.
448 33. Szklarczyk D, Gable AL, Lyon D, et al. 2019. STRING v11: protein-protein association
449 networks with increased coverage, supporting functional discovery in genome-wide
450 experimental datasets. Nucleic Acids Res 47:D607-d613.
451 34. Huang da W, Sherman BT, Lempicki RA. 2009. Systematic and integrative analysis of
452 large gene lists using DAVID bioinformatics resources. Nat Protoc 4:44-57.
453 35. Reich M, Liefeld T, Gould J, et al. 2006. GenePattern 2.0. Nat Genet 38:500-501.
454 36. Robinson JL, Soria P, Xu M, et al. 2018. Estrogen Promotes Mandibular Condylar
455 Fibrocartilage Chondrogenesis and Inhibits Degeneration via Estrogen Receptor Alpha in
456 Female Mice. Sci Rep 8:8527.

457 37. Grogan SP, Duffy SF, Pauli C, et al. 2018. Gene expression profiles of the meniscus
458 avascular phenotype: A guide for meniscus tissue engineering. J Orthop Res 36:1947-
459 1958.
460 38. Brophy RH, Zhang B, Cai L, et al. 2018. Transcriptome comparison of meniscus from
461 patients with and without osteoarthritis. Osteoarthritis Cartilage 26:422-432.
462 39. Muhammad H, Schminke B, Bode C, et al. 2014. Human migratory meniscus progenitor
463 cells are controlled via the TGF-β pathway. Stem Cell Reports 3:789-803.
464 40. Sun H, Wen X, Li H, et al. 2020. Single-cell RNA-seq analysis identifies meniscus
465 progenitors and reveals the progression of meniscus degeneration. Ann Rheum Dis
466 79:408-417.
467 41. Rovinski D, Ramos RB, Fighera TM, et al. 2018. Risk of venous thromboembolism
468 events in postmenopausal women using oral versus non-oral hormone therapy: A
469 systematic review and meta-analysis. Thromb Res 168:83-95.
470 42. Beral V. 2003. Breast cancer and hormone-replacement therapy in the Million Women
471 Study. Lancet 362:419-427.
472 43. Taylor HS, Manson JE. 2011. Update in hormone therapy use in menopause. J Clin
473 Endocrinol Metab 96:255-264.
474 44. Rothrauff BB, Yang G, Tuan RS. 2017. Tissue-specific bioactivity of soluble tendon-
475 derived and cartilage-derived extracellular matrices on adult mesenchymal stem cells.
476 Stem Cell Res Ther 8:133.
477 45. Tarafder S, Gulko J, Kim D, et al. 2019. Effect of dose and release rate of CTGF and
478 TGFβ3 on avascular meniscus healing. J Orthop Res 37:1555-1562.

479 46. Yuan X, Wei Y, Villasante A, et al. 2017. Stem cell delivery in tissue-specific hydrogel
480 enabled meniscal repair in an orthotopic rat model. Biomaterials 132:59-71.
481 47. Wang Q, Tan Q, Xu W, et al. 2018. Postnatal deletion of Alk5 gene in meniscal cartilage
482 accelerates age-dependent meniscal degeneration in mice. J Cell Physiol 234:595-605.
483 48. Valcourt U, Alcaraz LB, Exposito JY, et al. 2015. Tenascin-X: beyond the architectural
484 function. Cell Adh Migr 9:154-165.
485 49. Robertson IB, Horiguchi M, Zilberberg L, et al. 2015. Latent TGF-β-binding proteins.
486 Matrix Biol 47:44-53.
487 50. Son MS, Levenston ME. 2017. Quantitative tracking of passage and 3D culture effects on
488 chondrocyte and fibrochondrocyte gene expression. J Tissue Eng Regen Med 11:1185-
489 1194.
490

491 **Figure Legends**

492 **Figure 1:** Experimental design. Cells were isolated from the medial meniscus of two 47-year old
493 donors, one of each sex, and treated with two concentrations of E2 under pulsed and continuous
494 conditions. RNA-Seq was then used to analyze the samples. Running silhouettes from
495 freepik.com.

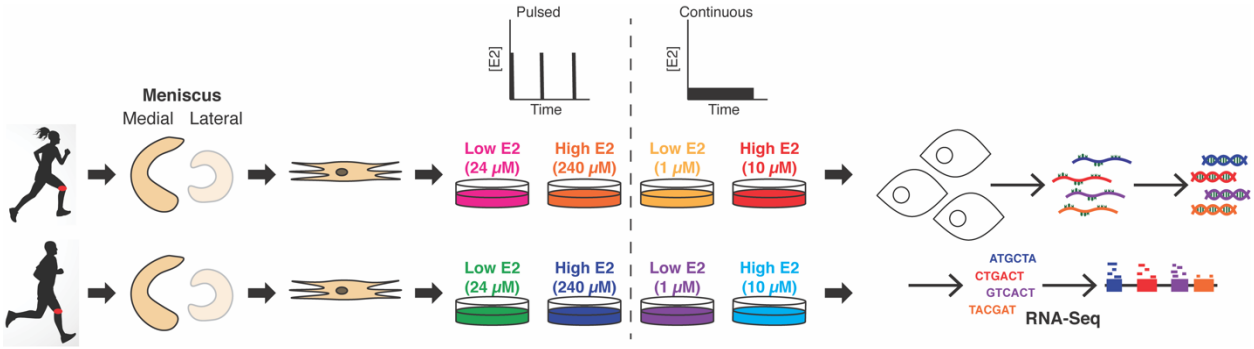

496

497

498 **Figure 2:** Visualization of the number of differentially expressed genes (DEGs) by treatment
499 group in comparison to physiological serum estrogen concentrations.

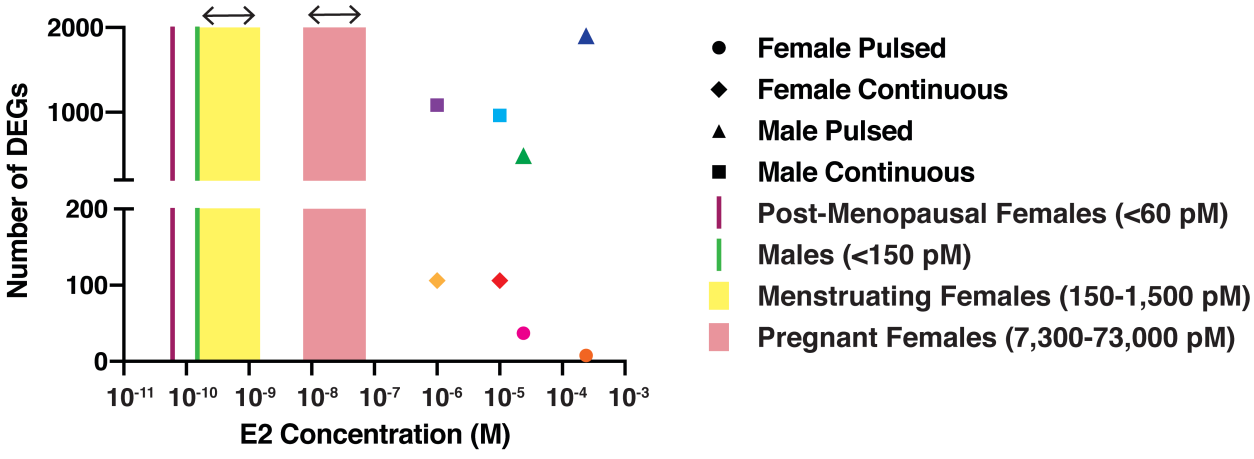

500

501

502 **Figure 3:** Visualization of differentially expressed genes (DEGs). Volcano plots and Venn
503 diagrams (Venny 2.1) illustrate the number of differentially expressed genes in each treatment
504 group. Only DEGs with padj<0.05 were used in the Venn diagrams.

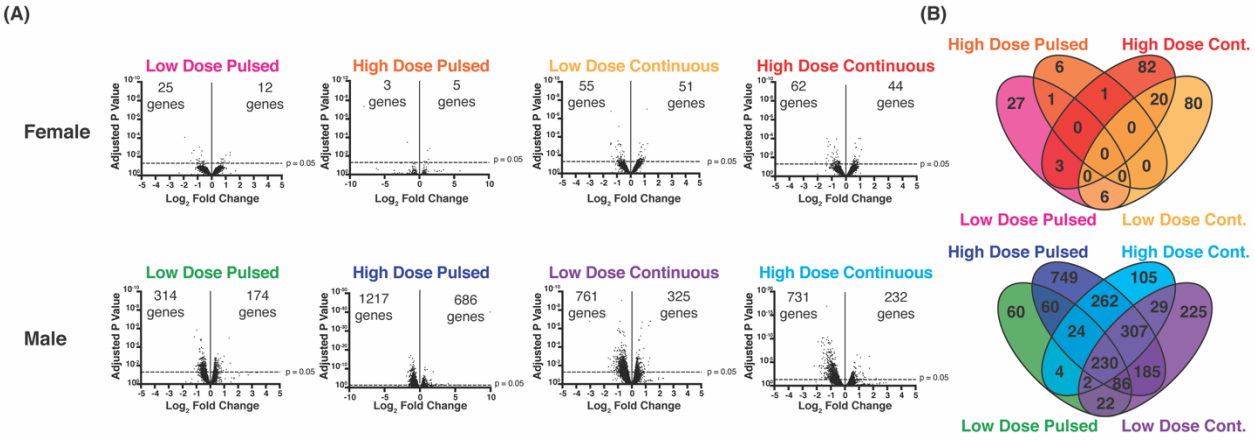

Figure 4: STRING analysis of DEGs from all 4 continuous dosing treatment groups. Images are shown as confidence views, where associations with stronger data support are thicker. Only DEGs with padj<0.05 are shown. Additional constraints based on log_2FoldChange were used to limit DEGs to a reasonable number for plotting and to highlight those with greater log_2FoldChanges. For the female groups, only log_2FoldChange >0.5 or <-0.5 are shown. For the male groups, only log_2FoldChange >1.0 or <-1.0 are shown. Color coding is based on functional enrichment analysis within STRING and is indicated for each treatment group. Abbreviations: GO-Gene Ontology, KEGG-Kyoto Encyclopedia of Genes and Genomes, ECM-extracellular matrix.

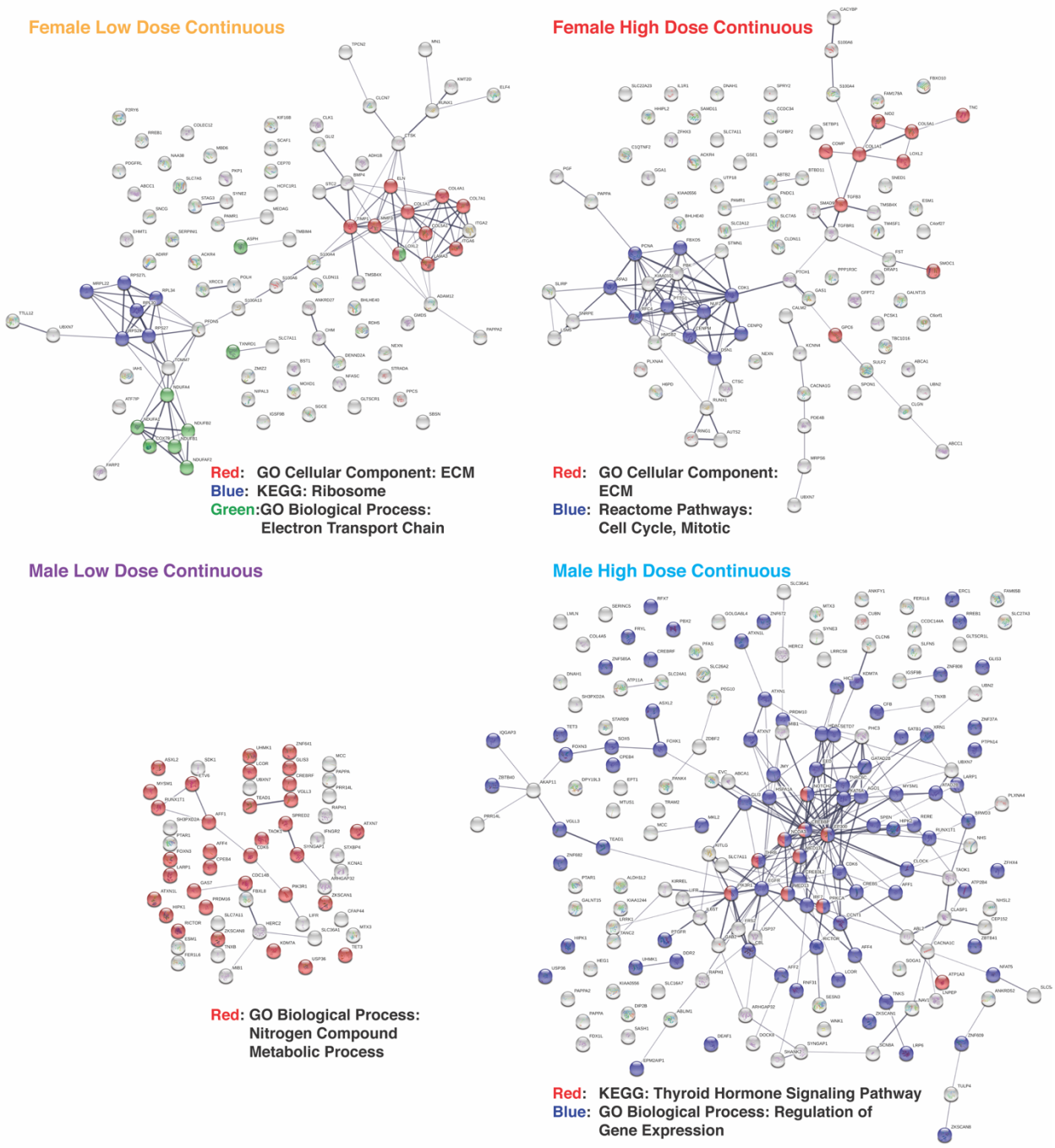

516

517

518 **Figure 5:** Analysis of the response of both sexes to the same treatment. (A) Venn diagrams

519 (Venny 2.1) were generated to show which genes were altered in both sexes under the same

520 treatment. For treatments with more than one common gene, functional enrichment analysis was

521 performed using (B) DAVID and (C) STRING analysis to determine what types of genes were
522 differentially expressed. Functional enrichment analysis shows the Gene Ontology Cellular
523 Component groups with p values<0.05. STRING analysis shows known and predicted
524 interactions between the proteins encoded by the genes in confidence views, where associations
525 with stronger data support are thicker.

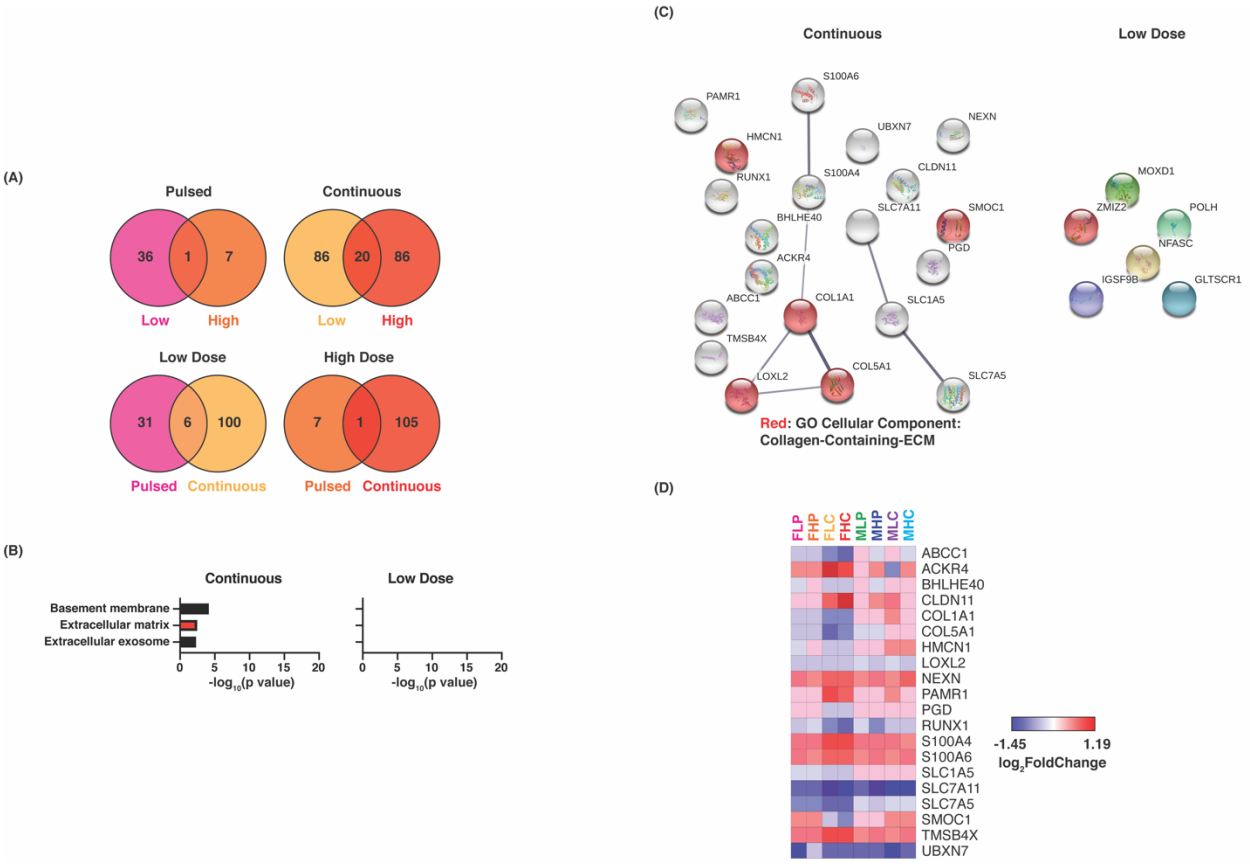

526

527

528 **Figure 6:** Analysis of DEGs that overlap between any two female treatment groups. (A) Venn
529 diagrams (Venny 2.1) were generated to show which genes were altered in more than one
530 treatment group. For groups with more than one common gene, functional enrichment analysis
531 was performed using (B) DAVID and (C) STRING analysis to determine what types of genes
532 were differentially expressed. (D) A heat map was generated of all 20 DEGs that were present in

both continuous treatment groups. Functional enrichment analysis shows the Gene Ontology Cellular Component groups with p values<0.05. STRING analysis shows known and predicted interactions between the proteins encoded by the genes in confidence views, where associations with stronger data support are thicker. Heat map was generated using GenePattern. Genes are listed in alphabetical order. Values shown are log_2FoldChange of each gene for each treatment group as compared to the sex-matched no E2 control.

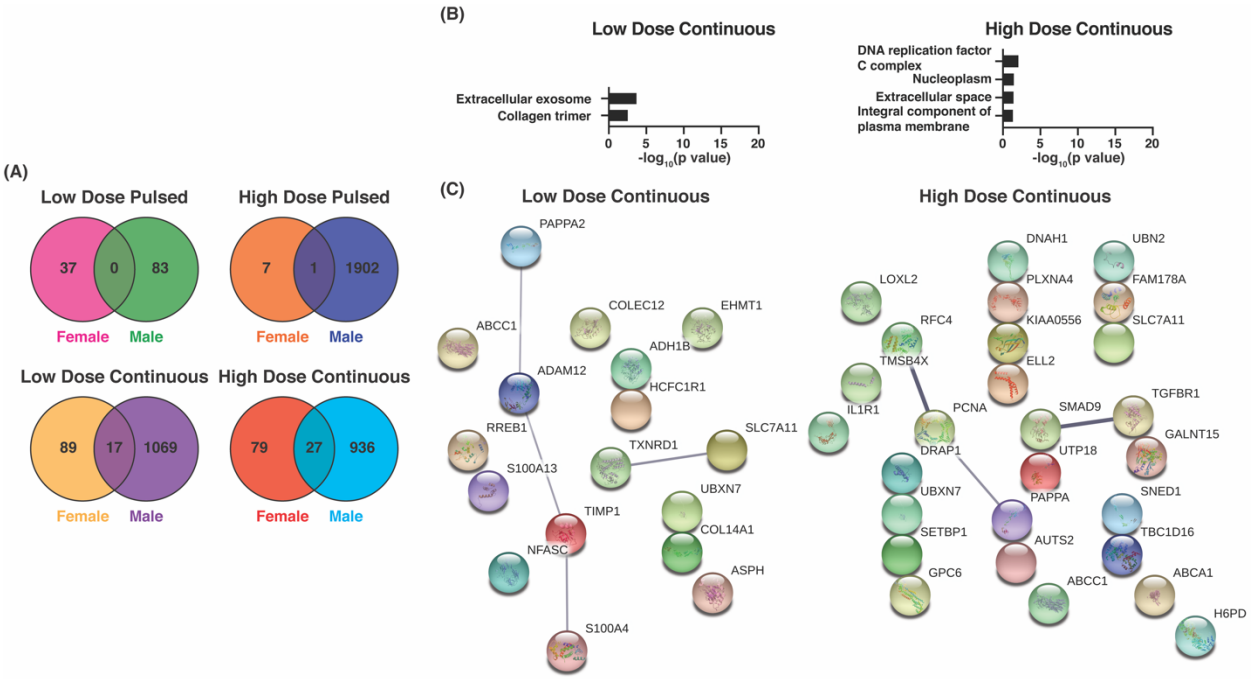

Figure 7: Functional enrichment analysis of DEGs using DAVID. Categories shown are from the Gene Ontology Cellular Component database. Where available, the top 15 groups by p value are shown with only p values < 0.05 considered.

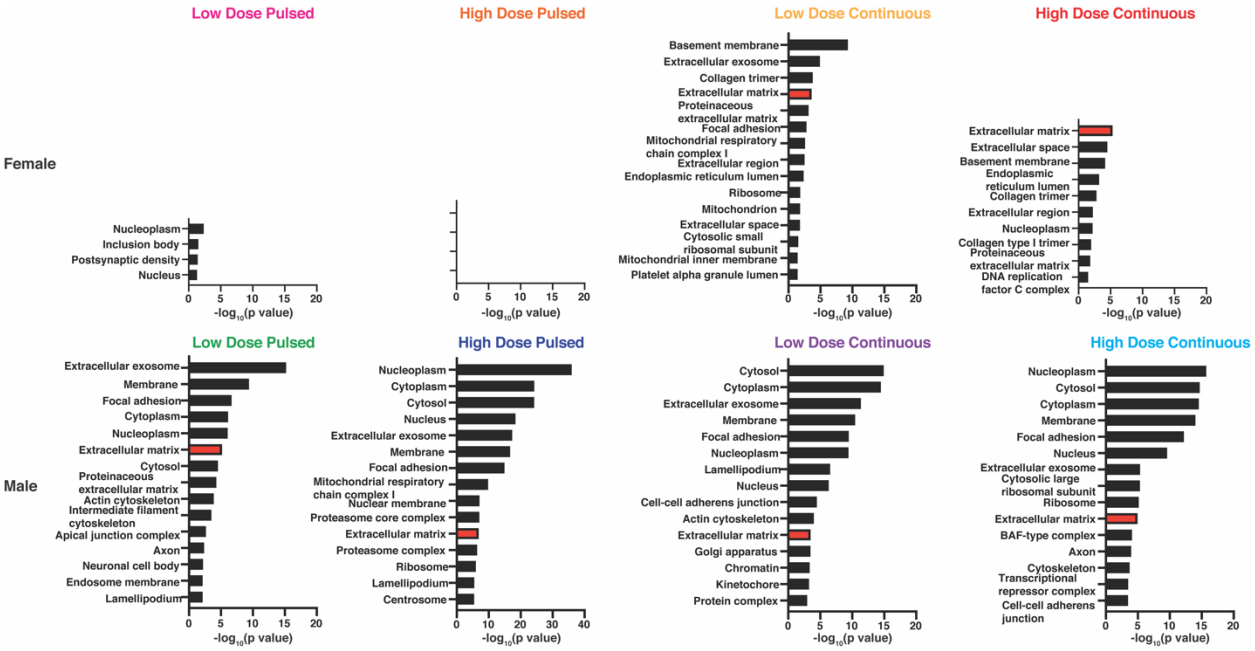

Figure 8: Heat map of extracellular matrix gene expression. Heat map was generated using GenePattern. Genes are listed in alphabetical order. Values shown are $\log_2$FoldChange of each gene for each treatment group as compared to the sex-matched no E2 control.

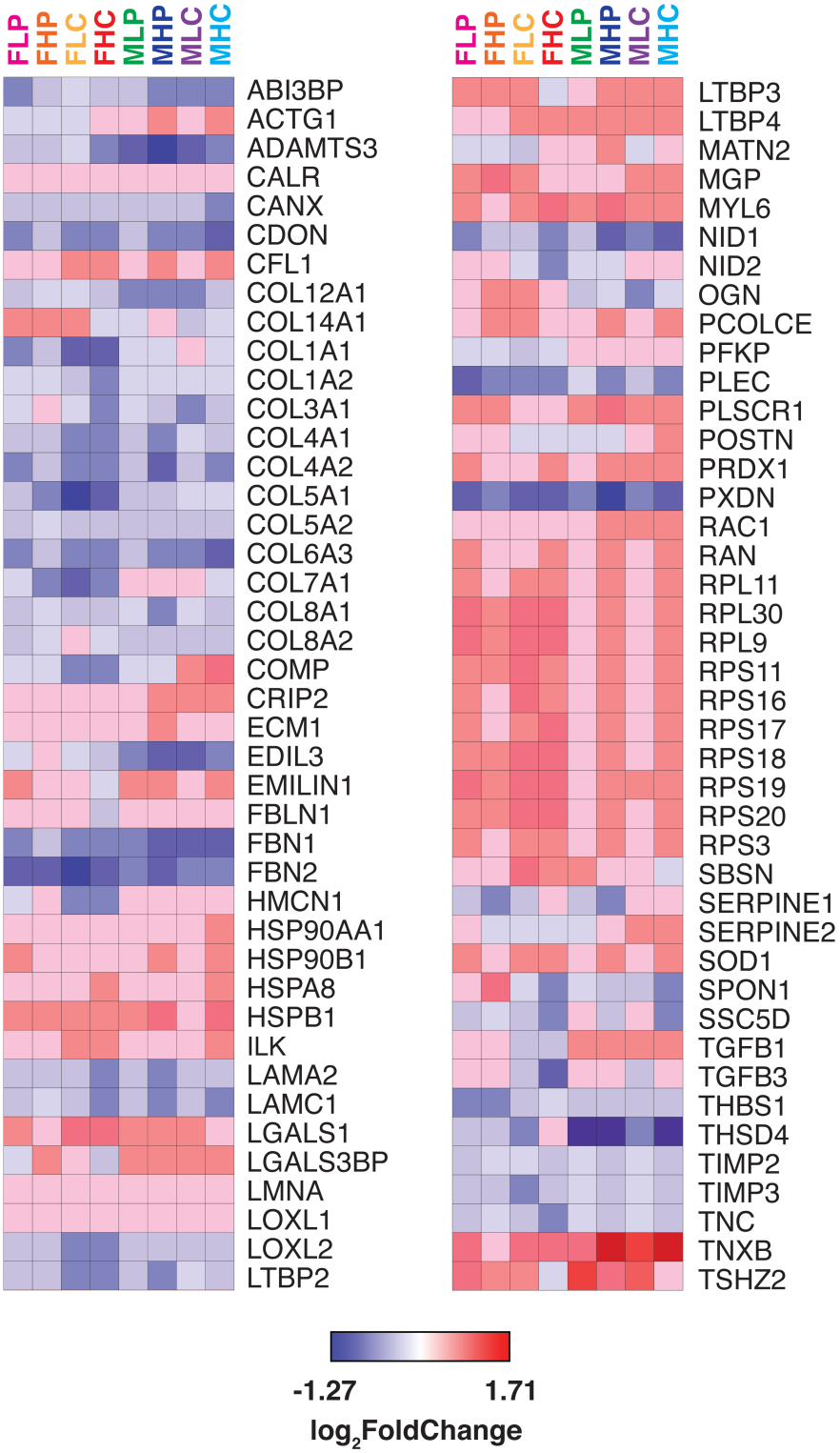
FLP
FHP
FLC
FHC
MLP
MHP
MLC
MHC
ABI3BP
ACTG1
ADAMTS3
CALR
CANX
CDON
CFL1
COL12A1
COL14A1
COL1A1
COL1A2
COL3A1
COL4A1
COL4A2
COL5A1
COL5A2
COL6A3
COL7A1
COL8A1
COL8A2
COMP
CRIP2
ECM1
EDIL3
EMILIN1
FBLN1
FBN1
FBN2
HMCN1
HSP90AA1
HSP90B1
HSPA8
HSPB1
ILK
LAMA2
LAMC1
LGALS1
LGALS3BP
LMNA
LOXL1
LOXL2
LTBP2
LTBP3
LTBP4
MATN2
MGP
MYL6
NID1
NID2
OGN
PCOLCE
PFKP
PLEC
PLSCR1
POSTN
PRDX1
PXDN
RAC1
RAN
RPL11
RPL30
RPL9
RPS11
RPS16
RPS17
RPS18
RPS19
RPS20
RPS3
SBSN
SERPINE1
SERPINE2
SOD1
SPON1
SSC5D
TGFB1
TGFB3
THBS1
THSD4
TIMP2
TIMP3
TNC
TNXB
TSHZ2
-1.27
1.71
log2FoldChange

549